

Non-equilibration of hydrostatic pressure in blebbing cells

Guillaume T. Charras¹, Justin C. Yarrow¹, Mike A. Horton², L. Mahadevan^{1,3,4} & T. J. Mitchison¹

Current models for **protrusive motility** in animal cells focus on cytoskeleton-based mechanisms, where localized protrusion is driven by **local regulation of actin biochemistry**^{1–3}. In plants and fungi, protrusion is driven primarily by hydrostatic pressure^{4–6}. For hydrostatic pressure to drive localized protrusion in animal cells^{7,8}, it would have to be locally regulated, but current models treating cytoplasm as an incompressible viscoelastic continuum⁹ or viscous liquid¹⁰ require that hydrostatic pressure equilibrates essentially instantaneously over the whole cell. Here, we use **cell blebs as reporters of local pressure in the cytoplasm**. When we locally perfuse blebbing cells with cortex-relaxing drugs to dissipate pressure on one side, blebbing continues on the untreated side, implying non-equilibration of pressure on **scales of approximately 10 μm and 10 s**. We can account for localization of pressure by considering the **cytoplasm as a contractile, elastic network infiltrated by cytosol**. Motion of the fluid relative to the network generates spatially heterogeneous transients in the pressure field, and can be described in the framework of poroelasticity^{11,12}.

Blebs are large, approximately spherical deformations of the cell surface that form and disappear on a timescale of tens of seconds.

Although less studied than lamellipodial or filopodial protrusion, blebbing is a common phenomenon during apoptosis¹³, cytokinesis^{14,15} and cell movement^{16,17}. Blebs are thought to be initiated by rupture of the plasma membrane from the underlying cytoskeleton (Supplementary Fig. 3), followed by inflation of the detached membrane by intracellular fluid flow^{18,19}. Subsequent bleb retraction is driven by assembly and contraction of a cortex within the newly formed bleb. Blebbing requires non-uniform behaviour of the membrane and cortex that must reflect either a globally uniform hydrostatic pressure combined with local nucleation of membrane detachment from the cytoskeleton, or non-uniform pressure leading to local rupture of membrane–cytoskeleton attachments in regions of high pressure. To distinguish these possibilities, we studied the effect of local disruption of cortical contraction or integrity induced by drug perfusion over part of a cell, in a filamin-depleted melanoma cell line (M2) that blebs extensively and continuously²⁰.

We first confirmed that the cell volume stays approximately constant during blebbing (Supplementary Data, Supplementary Video 12 and Supplementary Fig. 4)¹⁸, implying that blebbing is driven primarily by flow of fluid within the cell rather than water crossing the plasma membrane. We then confirmed that bleb inflation represents ballooning out of the plasma membrane when it detaches from the actin cortex by simultaneously imaging the cortex and the cell membrane (Supplementary Fig. 3). During bleb inflation, green fluorescent protein (GFP)-tagged actin was not enriched at the bleb surface compared to its interior, implying lack of a cytoskeleton in the bleb (Fig. 1a, $t = 0$ and 22 s). As inflation slowed, a cortical cytoskeleton assembled underneath the bleb membrane, evidenced by a rim of actin fluorescence (Fig. 1a,

$t = 62$ s); simultaneously, the cortex at the base of the bleb disassembled (Supplementary Fig. 3). As the bleb retracted, its actin rim became more pronounced, and often wavy or buckled, suggesting that the cortex contracts as the bleb shrinks (Fig. 1a, $t = 72$ s)¹⁹. GFP–myosin II regulatory light chain (MRLC) was recruited to the newly forming cortex of the bleb simultaneous with actin (Fig. 1b; see also Supplementary Video 10)^{13,21}, consistent with myosin II driving contraction. Increasing extracellular osmolarity made blebs smaller, whereas decreasing it made them larger²² (Fig. 1; see also Supplementary Video 1). Increasing membrane rigidity by crosslinking the glycocalyx polysaccharides with wheat germ agglutinin (WGA)²³ inhibits blebbing (Supplementary Video 2). These observations, together with drug studies discussed below, support the following qualitative model for bleb dynamics¹⁹. Cortical acto-myosin contracts (Supplementary Videos 10 and 11), generating hydrostatic pressure that causes a patch of plasma membrane to tear free from its attachment to the cortical cytoskeleton. This patch of cytoskeleton-free membrane rapidly inflates as cytosol flows in, with its base enlarging by further tearing (Supplementary Fig. 3). Later, inflation slows and a mesh of actin and myosin II assembles in the bleb to form a contractile cortex attached to the plasma membrane (Fig. 1b). Finally, contraction of this cortical mesh causes the bleb to shrink, driving the extruded cytosol back into the cell body.

To find inhibitory small molecules, we screened a library of known biologically active compounds for rapid inhibition of blebbing. After characterizing their effects in bath treatment, selected drugs and osmolytes were applied locally to cells by injecting medium containing inhibitor via a micropipette into a laminar fluid flow^{24,25}. The treated region was visualized by adding a fluorescent tracer to the pipette medium, whereas blebbing was observed using differential interference contrast (DIC) microscopy. During local perfusion, we typically bathed 20–33% of the cell area. We confirmed local application by visualizing local deposition of a fluorescent lectin (WGA–Alexa 488; Fig. 2a, $t = 430$ s). For each drug, local perfusion experiments were repeated until one of the following behaviours was observed reproducibly ($N \geq 5$): (1) local perfusion of drug inhibited blebbing locally; (2) local perfusion had both a local and global effect on blebbing; (3) local perfusion did not inhibit blebbing but whole-cell treatment did.

The effect of local perfusion could be classified into three categories. The first is treatments that locally inhibited blebbing but allowed the untreated part of the cell to bleb normally (Fig. 2; see also Supplementary Table 1 and Supplementary Videos 3–6). As expected, agents that increased membrane rigidity (WGA) or osmotic pressure (sucrose) had this effect (Fig. 2a, b). These agents locally increase the physical forces that oppose blebbing. Notably, drugs that block generation of contractile force also had local inhibitory effects, including inhibitors of myosin II (blebbistatin²¹) and ROCK1 (Y-27632 and 3-(4-pyridyl)indole²⁶), a kinase that activates

¹Department of Systems Biology, Harvard Medical School, Boston, Massachusetts 02115, USA. ²London Centre for Nanotechnology, University College London, London WC1E 6JF, UK. ³Division of Engineering and Applied Sciences, and ⁴Department of Organismic and Evolutionary Biology, Harvard University, Cambridge, Massachusetts 02138, USA.

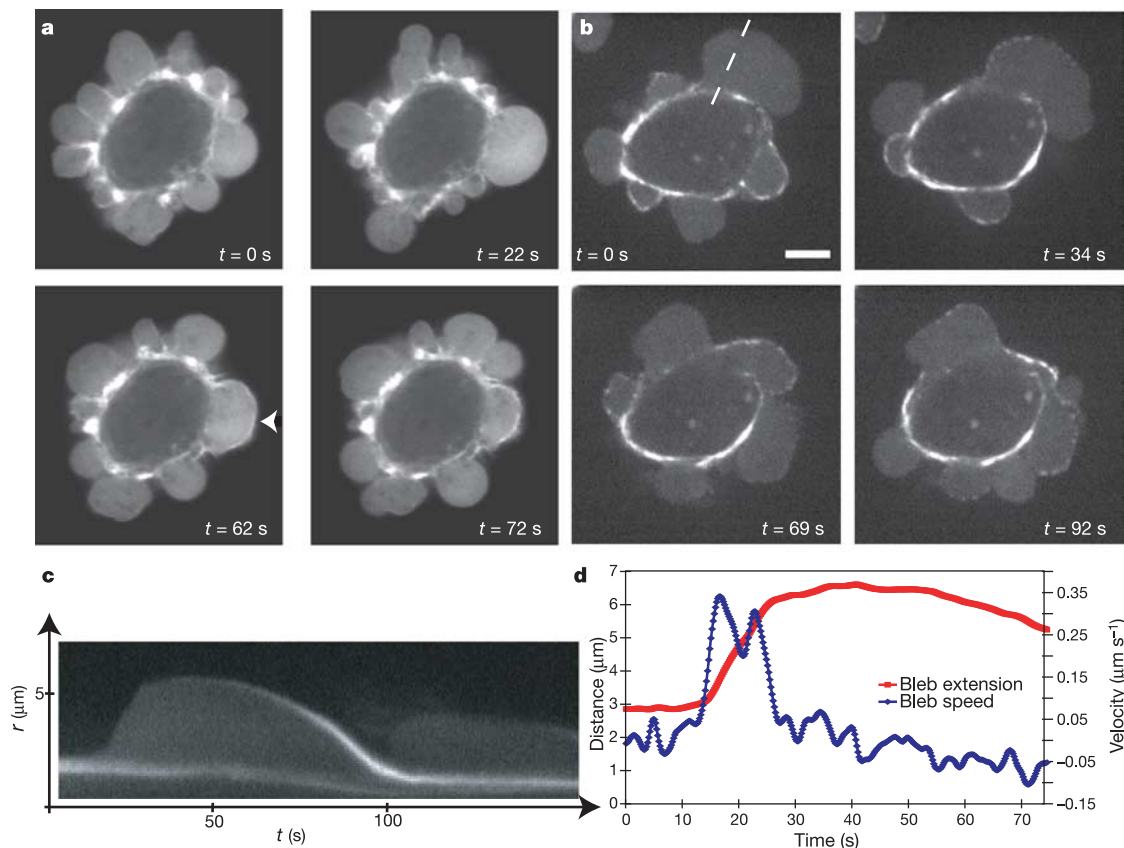


Figure 1 | Localization of GFP-actin and GFP-MRLC in blebs shows that expansion is a passive process and retraction an active process necessitating actin and MRLC. All images were acquired by confocal microscopy. Scale bar, 5 μm . **a**, GFP-actin-transfected cell. During bleb expansion, the bleb rim does not appear to be enriched in GFP-actin compared to the bleb interior ($t = 0$ s and $t = 22$ s). Once expansion has halted, an actin-rich rim forms at the bleb surface ($t = 62$ s, arrowhead) and retraction begins. As retraction proceeds, the actin rim becomes wavy, suggesting that the cortex contracts as the bleb shrinks ($t = 72$ s). **b**, GFP-MRLC-transfected cell. Just after expansion has stopped, the bleb surface

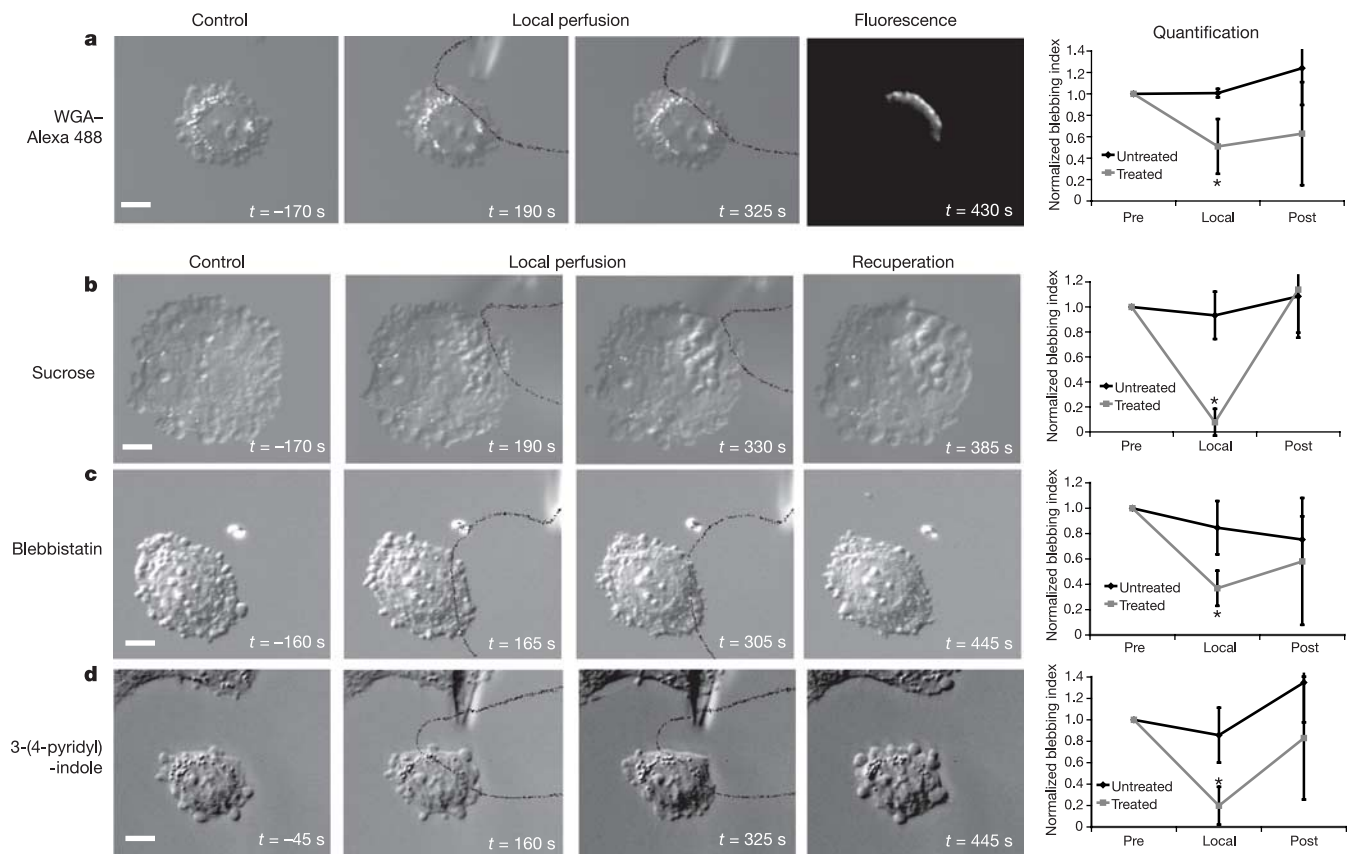
does not appear to be enriched in GFP-MRLC ($t = 0$ s). MRLC then accumulates in discrete foci ($t = 34$ s) and retraction starts ($t = 69$ s). As retraction ends, MRLC forms a continuum along the bleb rim ($t = 92$ s). **c**, Kymograph of the expansion and retraction of the bleb in **b** (dashed line). As the bleb expands, there is no accumulation of MRLC at the bleb apex. As retraction proceeds, MRLC accumulates at the bleb. Bleb extension (r) is on the y axis. **d**, Graph of the bleb extension and bleb velocity as a function of time for the bleb shown in **c**. The maximal bleb extension is approximately 3.5 μm (maximal speed of expansion about $0.35 \mu\text{m s}^{-1}$, speed of retraction about $0.1 \mu\text{m s}^{-1}$).

myosin II (Fig. 2c, d). The second category is treatments that caused a combination of local and global effects, as seen with the F-actin-disrupting agents cytochalasin D and latrunculin B (Fig. 3a; see also Supplementary Video 7). Within seconds of local drug application, there was a global increase in bleb size (Fig. 3a, $t = 75$ s). Then, blebbing ceased in the treated area and existing blebs were not retracted, whereas blebbing continued in the untreated area at a slower rate than before drug application (Fig. 3a, $t = 315$ s). The third category is treatments that only had an effect when the whole cell was treated. Inhibitors of several other protein kinases had this effect (Fig. 3b, c; see also Supplementary Videos 8 and 9). For local perfusion to perturb the cytoplasm locally, membrane crossing must be fast compared with intracellular diffusion of the drug or drug-target complex²⁷. Thus, failure to see a local effect of a drug cannot be interpreted in terms of local versus global action of its target.

The local effects of myosin-II-inhibiting drugs (Fig. 2c, d) show that the acto-myosin cortex acts locally to promote blebbing. This could be because contraction locally nucleates blebs, while hydrostatic pressure is uniform, or because pressure generated by contraction only acts locally to extrude blebs, implying that it does not globally equilibrate. Local inhibition of blebbing by actin-depolymerizing drugs (Fig. 3a) favours the latter hypothesis. If pressure equilibrated across the cell, the drug-treated side, where the cortex is softer, should swell preferentially, inhibiting blebbing on

the untreated side. Because this does not happen, we conclude that hydrostatic pressure does not equilibrate across single M2 cells on time- and length-scales relevant to motility.

Current models of the cytoplasm^{9,10} cannot account for spatio-temporally localized variations in hydrostatic pressure. We therefore propose a new description of the cytoplasm based on poroelasticity^{11,12}. We consider the cytoplasm to be composed of a porous, actively contractile, elastic network (cytoskeletal filaments, organelles and ribosomes), infiltrated with an interstitial fluid (that is, the cytosol, comprising water, ions and soluble proteins), similar to a fluid-filled sponge. Contraction of the acto-myosin cortex creates a compressive stress on the cytoskeletal network, leading to a spatially localized increase in hydrostatic pressure (Fig. 4a). In response, the cytosol flows out of the network, and if it finds a region where the membrane is weakly attached to the cortex; the resulting pressure can lead to membrane detachment and bleb inflation (Fig. 4b; see also Supplementary Fig. 3). With a poroelastic description of the cytoplasm, hydrostatic pressure does not instantaneously propagate through the network. Instead, it diffuses over a length $x \approx \sqrt{Dt}$ during a time t , with the diffusion constant $D = \frac{kK}{\phi}$ determined by an appropriately defined elastic bulk modulus K , the hydraulic permeability of the network k , and the local volume fraction of fluid ϕ (see Supplementary Information). The diffusion constant D dictates the time needed for the effect of a local contractile force to be felt in



myosin II ATPase by local perfusion of blebbistatin. **d**, Local inhibition of ROCK1 by 3-(4-pyridyl)indole. Black lines delineate the flow out of the micropipette. On each image, timing relative to local application of treatment is given. The normalized blebbing indices (right) show the evolution over time of blebbing in the region exposed to inhibitor and in the free region. Error bars show the standard deviation. Asterisks denote significant changes in the blebbing index when compared with the initial blebbing index. Scale bars, 10 μm .

other parts of the cell. Using a typical timescale for bleb inflation of $t \approx 10$ s and realistic values for the various parameters (Supplementary Information), we find $x \approx 15\text{--}30$ μm . Hence, hydrostatic pressure can be strongly non-equilibrated in cells on a timescale of approximately 10 s and a length scale of about 10 μm —scales that are relevant to a variety of motile behaviours. Bleb formation reduces this length scale by allowing the fluid to flow, with less resistance, into the blebs instead of through the network. Local inhibition of blebbing is possible because opposite sides of the cells are effectively isolated from each other with respect to equilibration of pressure on a timescale of seconds.

Our poroelastic model could have important implications for other types of cell motility, because it implies that hydrostatic pressure can be generated and used locally to power shape change in animal cells. Leading-edge protrusion is typically coupled to actin polymerization^{1–3}, but hydrodynamic force could work together with polymerization force to power protrusion^{7,8}, and fluid flow could drive actin subunits forwards at a faster rate than that predicted by pure diffusion²⁸. Localized hydrostatic pressure transients could be generated locally near the front of polarized cells by local recruitment and activation of myosin II as in blebbing, or of plasma membrane ion transporters (such as NHE1 (ref. 29)) that can trigger swelling through influx of an osmolyte (such as Na^+). Overall, our work shows that cytosolic fluid dynamics must be integrated with protein dynamics if we are to really understand cell motility.

METHODS

Local perfusion. Local perfusion was performed by injecting medium with the desired concentration of drug into a laminar fluid flow via a glass micropipette with a 1–2- μm diameter. Thin-walled borosilicate micropipettes (0.9-mm inner diameter) were pulled on a Sutter P87 pipette puller (Sutter instrument company). Coverslips on which cells had been cultured were affixed onto the bottom of the laminar fluid flow chamber (blueprint available upon request) with a 1:1:1 mix of vaseline, lanolin and paraffin. Laminar flow was created by feeding medium into the flow chamber at a constant rate of 30 ml h^{-1} with a syringe pump. A constant fluid level was maintained by aspirating the supernatant via a vacuum pump. The flow chamber consisted of a reservoir with a small opening (0.7 mm) that enables medium to enter the open part of the chamber and delivers a flow of approximately 30 $\mu\text{m s}^{-1}$ in the vicinity of this entrance. For the flow to be sufficiently rapid to carry drug away, the target cells needed to be chosen within 200 μm of the reservoir opening. All experiments were performed at room temperature in Leibovitz-L15 medium with 10% 80:20 mix of donor calf serum:fetal calf serum. The microinjected solution was made up of medium with the desired concentration of drug and 0.1 μM of tetramethylrhodamine-isothiocyanate (TRITC, used as a fluorescent tracer) and filtered using a centrivic tube (Millipore). The micropipettes were backfilled with the solution and mounted onto a pipette holder attached to a three-axis oil hydraulic micromanipulator (Narishige). A pressure regulator (Eppendorf 5242, Eppendorf AG) set between 40 and 80 hPa was used to control flow from the micropipette.

Time-lapse video microscopy of the local perfusion experiments was performed as described in Supplementary Methods, except that in addition to DIC images, fluorescence images were also acquired (TRITC filters to visualize flow lines and fluorescein-isothiocyanate (FITC) filters to visualize WGA–Alexa

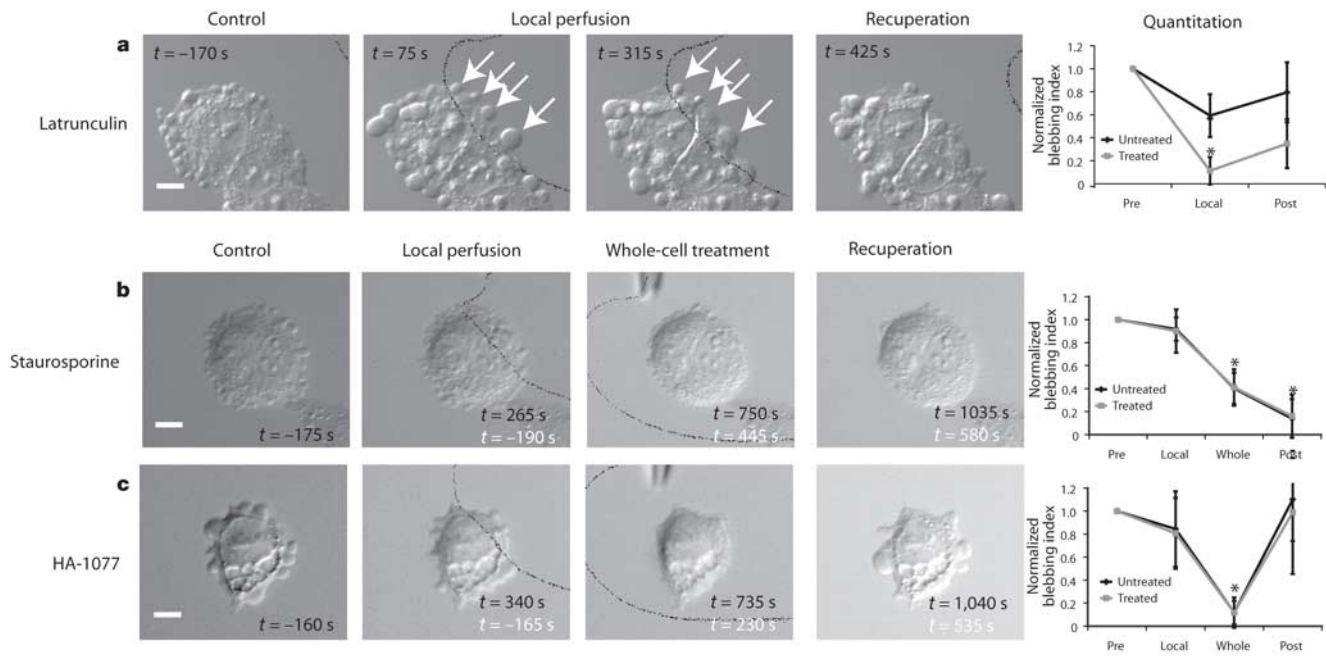


Figure 3 | Compounds with dual or global effects on blebbing. **a**, Local perfusion with latrunculin B has a dual effect. When latrunculin B is applied locally, bleb size increases globally ($t = 75$ s), and bleb dynamics cease in the treated area ($t = 75$ s and $t = 315$ s). Elsewhere, expansion and retraction continue. **b**, Global perfusion of staurosporine is necessary to inhibit blebbing. Before perfusion ($t = -175$ s) and after 395 s of local perfusion with staurosporine, blebbing is unperturbed throughout the cell. When staurosporine is applied to the whole cell (white text, $t = 445$ s), blebbing ceases. **c**, Global perfusion of HA-1077 is necessary to inhibit blebbing. After 340 s of local HA-1077 application, blebbing is unperturbed. When the

whole cell is exposed to inhibitor ($t = 230$ s, white text), blebbing ceases. When perfusion is halted, blebbing is restored ($t = 535$ s, white text). Black lines delineate the flow coming out of the micropipette. Black text gives time relative to local application; white text gives time relative to global application. The normalized blebbing indices show the evolution over time of blebbing in the region exposed to inhibitor and in the free region. Error bars show the standard deviation. Asterisks denote significant changes in the blebbing index when compared with the initial blebbing index. Scale bars, 10 μ m.

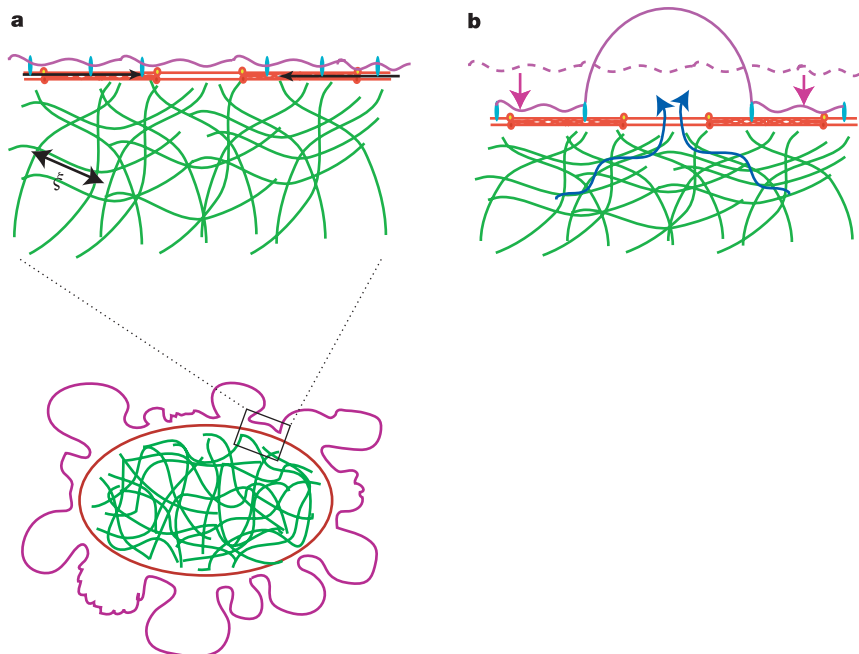


Figure 4 | Poroelastic description of blebbing. In all drawings, the actin cortex is drawn in red, the membrane is mauve and the cytoskeletal meshwork is green. **a**, In blebbing cells, a local contraction of myosin II (black arrows) associated with the actin cortex leads to a shortening of the cortical periphery and therefore to a compression of the cytoskeletal network that fills the cell. The cytoskeletal network is porous and has an average pore size ξ . The compression of the cytoskeletal meshwork creates a hydrostatic

pressure in the vicinity of the region of contraction and can lead to bleb nucleation and expansion. **b**, Contraction of the actin cortex leads to a compression of the cytoskeletal network (the dashed mauve line indicates the original position of the cell surface) and drives flow of cytosol in the opposite direction (blue arrows). If there is a local defect in membrane-cytoskeleton attachment, a bleb is extruded. Bleb expansion is opposed by two forces: extracellular osmotic pressure and membrane tension.

488). Exposure times were approximately 200 ms for DIC images, 600 ms for TRITC images and about 250 ms for FITC images. Images were acquired every 5 s with a $\times 20$ objective using Metamorph (Universal Imaging Corp.). During a typical local perfusion experiment, about 30 images (approximately 150 s) were acquired before drug exposure. Then, the cell was exposed to drug for about 70 images (approximately 350 s), finally the cell was allowed to recover for 20 frames (about 100 s). When no local inhibition was observed, a whole-cell treatment was performed. This time, the cell was observed for 30 frames to ensure that it still blebbed, the whole cell was exposed to drug for 70 frames, and recovered for 20 frames. Initial concentrations of drug in the microinjected fluid were chosen to be two to three times those needed in bulk solution²⁵. When no inhibition was observed when the whole cell was exposed to drug, the drug concentration in the micropipette was increased. When whole-cell inhibition was observed with only local perfusion, the drug concentration was decreased.

Post-hoc flow lines were superimposed onto the DIC images using Metamorph. The fluorescence images were assigned a threshold and intensities of 25% of the maximum intensity were converted to a binary image that was inverted and superimposed onto the DIC image using an AND operator.

Analysis and quantification of local perfusion assays. Each cell was divided into two regions: the treated region where local perfusion was applied, and the control untreated region. Each experiment was divided into different periods: (1) before the application of drug; (2) during local application of drug; (3) after application of drug; and, if need be, (4) during whole-cell treatment. The number of blebs occurring in each region for each period was counted manually. A blebbing index was computed for each region as follows: $B = \frac{N_{\text{blebs}}}{Lt}$, where N_{blebs} is the number of blebs observed during a given period t over a given perimeter L . These blebbing indices were used to compare the treated region to the untreated region before application of inhibitor, and the blebbing in either region during and after application of inhibitor to the blebbing in that region before application. Populations were compared with a Student's t -test and the level of significance was taken to be $P < 0.01$. For graphic output (Figs 2 and 3), the evolution of the blebbing indices was normalized to their values before application of local perfusion. In all cases, the blebbing index in the treated and untreated region was not significantly different before application of inhibitor ($P > 0.3$).

Received 19 January; accepted 15 March 2005.

- Mahadevan, L. & Matsudaira, P. Motility powered by supramolecular springs and ratchets. *Science* **288**, 95–100 (2000).
- Rafelski, S. M. & Theriot, J. A. Crawling toward a unified model of cell mobility: spatial and temporal regulation of actin dynamics. *Annu. Rev. Biochem.* **73**, 209–239 (2004).
- Mogilner, A. & Oster, G. Polymer motors: pushing out the front and pulling up the back. *Curr. Biol.* **13**, R721–R733 (2003).
- Messerli, M. A. & Robinson, K. R. Ionic and osmotic disruptions of the lily pollen tube oscillator: testing proposed models. *Planta* **217**, 147–157 (2003).
- Money, N. P. & Harold, F. M. Extension growth of the water mold *Achlya*: interplay of turgor and wall strength. *Proc. Natl Acad. Sci. USA* **89**, 4245–4249 (1992).
- Harold, F. M. Force and compliance: rethinking morphogenesis in walled cells. *Fungal Genet. Biol.* **37**, 271–282 (2002).
- Tilney, L. G. & Inoue, S. Acrosomal reaction of the Thyone sperm. III. The relationship between actin assembly and water influx during the extension of the acrosomal process. *J. Cell Biol.* **100**, 1273–1283 (1985).
- Condeelis, J. Life at the leading edge: the formation of cell protrusions. *Annu. Rev. Cell Biol.* **9**, 411–444 (1993).
- Boal, D. H. *Mechanics of the Cell* (Cambridge Univ. Press, Cambridge, UK, 2002).
- Drury, J. L. & Dembo, M. Hydrodynamics of micropipette aspiration. *Biophys. J.* **76**, 110–128 (1999).
- Biot, M. General theory of three-dimensional consolidation. *J. Appl. Phys.* **12**, 155–164 (1941).
- Wang, H. *Theory of Linear Poroelasticity with Applications to Geomechanics and Hydrogeology* (Princeton Univ. Press, Princeton, New Jersey, 2000).
- Mills, J. C., Stone, N. L., Erhardt, J. & Pittman, R. N. Apoptotic membrane blebbing is regulated by myosin light chain phosphorylation. *J. Cell Biol.* **140**, 627–636 (1998).
- Fishkind, D. J., Cao, L. G. & Wang, Y. L. Microinjection of the catalytic fragment of myosin light chain kinase into dividing cells: effects on mitosis and cytokinesis. *J. Cell Biol.* **114**, 967–975 (1991).
- Burton, K. & Taylor, D. L. Traction forces of cytokinesis measured with optically modified elastic substrata. *Nature* **385**, 450–454 (1997).
- Trinkaus, J. P. Surface activity and locomotion of *Fundulus* deep cells during blastula and gastrula stages. *Dev. Biol.* **30**, 69–103 (1973).
- Friedl, P. & Wolf, K. Tumour-cell invasion and migration: diversity and escape mechanisms. *Nature Rev. Cancer* **3**, 362–374 (2003).
- Albrecht-Buehler, G. Does blebbing reveal the convulsive flow of liquid and solutes through the cytoplasmic meshwork? *Cold Spring Harb. Symp. Quant. Biol.* **46**, 45–49 (1982).
- Cunningham, C. C. Actin polymerization and intracellular solvent flow in cell surface blebbing. *J. Cell Biol.* **129**, 1589–1599 (1995).
- Cunningham, C. C. *et al.* Actin-binding protein requirement for cortical stability and efficient locomotion. *Science* **255**, 325–327 (1992).
- Cheung, A. *et al.* A small-molecule inhibitor of skeletal muscle myosin II. *Nature Cell Biol.* **4**, 83–88 (2002).
- Dai, J. & Sheetz, M. P. Membrane tether formation from blebbing cells. *Biophys. J.* **77**, 3363–3370 (1999).
- Evans, E. & Leung, A. Adhesivity and rigidity of erythrocyte membrane in relation to wheat germ agglutinin binding. *J. Cell Biol.* **98**, 1201–1208 (1984).
- Popov, S., Brown, A. & Poo, M. M. Forward plasma membrane flow in growing nerve processes. *Science* **259**, 244–246 (1993).
- O'Connell, C. B., Warner, A. K. & Wang, Y. Distinct roles of the equatorial and polar cortices in the cleavage of adherent cells. *Curr. Biol.* **11**, 702–707 (2001).
- Yarrow, J. C., Totsukawa, G., Charras, G. T. & Mitchison, T. J. Screening for cell migration inhibitors via automated microscopy reveals a rho-kinase inhibitor. *Chem. Biol.* **12**, 385–395 (2005).
- Takayama, S. *et al.* Selective chemical treatment of cellular microdomains using multiple laminar streams. *Chem. Biol.* **10**, 123–130 (2003).
- Zicha, D. *et al.* Rapid actin transport during cell protrusion. *Science* **300**, 142–145 (2003).
- Baumgartner, M., Patel, H. & Barber, D. L. Na(+)/H(+) exchanger NHE1 as plasma membrane scaffold in the assembly of signaling complexes. *Am. J. Physiol. Cell Physiol.* **287**, C844–C850 (2004).

Supplementary Information is linked to the online version of the paper at www.nature.com/nature.

Acknowledgements The authors would like to acknowledge the Nikon Imaging Centre at Harvard Medical School and, in particular, J. Waters. The authors would also like to acknowledge J. Horn at the HMS machine shop for manufacturing the perfusion chamber. G.T.C. was in receipt of a Wellcome Trust Overseas Fellowship. M.A.H. is supported by a Programme Grant from the Wellcome Trust. L.M. was supported by NSF-MRSEC at Harvard University. This work was supported by a grant from the NIH to T.J.M.

Author Information Reprints and permissions information is available at npg.nature.com/reprintsandpermissions. The authors declare no competing financial interests. Correspondence and requests for materials should be addressed to G.T.C. (gcharras@hms.harvard.edu).